The Journal of Experimental Biology 214, 703-708

doi:10.1242/jeb.051144

METHODS & TECHNIQUES

Dynamics of gecko locomotion: a force-measuring array to measure 3D reaction forces

Zhendong Dai*, Zhouyi Wang and Aihong Ji

Institute of Bio-inspired Structure and Surface Engineering, Nanjing University of Aeronautics and Astronautics, Nanjing, 210016, People's Republic of China

*Author for correspondence (zddai@nuaa.edu.cn)

Accepted 16 November 2010

SUMMARY

Measuring the interaction between each foot of an animal and the substrate is one of the most effective ways to understand the dynamics of legged locomotion. Here, a new facility – the force-measuring array (FMA) – was developed and applied to measure 3D reaction forces of geckos on different slope surfaces. The FMA consists of 16 3D sensors with resolution to the mN level. At the same time the locomotion behaviour of geckos freely moving on the FMA was recorded by high speed camera. The reaction forces acting on the gecko's individual feet measured by the FMA and correlated with locomotion behaviour provided enough information to reveal the mechanical and dynamic secrets of gecko locomotion. Moreover, dynamic forces were also measured by a force platform and correlated with locomotion behaviour. The difference between the forces measured by the two methods is discussed. From the results we conclude that FMA is the best way to obtain true reaction forces acting on the gecko's individual feet.

Key words: force-measuring array (FMA), 3D reaction force, force platform, gecko.

INTRODUCTION

Any change of motion of an object results from force acting on it, as does the motion of animals. Animal locomotion seems simple – an organism exerts a force on the external environment and, through Newton's third law, a reaction force from the environment acts on the animal and accelerates the motion (Dickinson et al., 2000). However, studies indicate that the spatial and temporal dynamics of force application are not as simple as they first appear, so measurement of the interactive forces between an organism and the environment becomes one of the most effective approaches to understanding the locomotion of animals. A vast amount of data on interactive forces has accumulated over the years. Various methods of measuring the force acting on individual limbs have been developed. A buckle force transducer was developed which could be implanted into a tendon to measure the force generated by muscle directly (Biewener et al., 1988; Kleinrensink et al., 2000; Nikanjam et al., 2007). Unfortunately this approach may wear and damage the tendon and results in unpredictable changes in the locomotion behaviour and dynamics, so it has not been widely used in recent years. Wearable force sensors were developed to measure the vertical ground reaction force of horses (Kai et al., 2000; Merkens et al., 1986) and the normal and shear forces of humans (Liu et al., 2007). This method is relatively cheap because only a small number of sensors are used, and the reaction forces of many consecutive strides can be measured, but it is not suitable for measuring the reaction force generated by geckos and other sticky animals, because a wearable sensor cannot generate adhesive force like a gecko. A force platform was first introduced by Manter in 1938; he measured the 3D reaction force of a cat moving on a horizontal substrate by observing the displacement of three springs, which were used to hang the substrate (Manter, 1938). Many researchers have developed 2D mini force platforms to measure the reaction force of various animals, when the animals move on horizontal or vertical substrates (Biewener et al., 1988; Blickhan et al., 1987; Herzog et al., 1989; Full and Tu, 1990; Heglund, 1981). However, the force measured by the 2D mini force platform cannot completely reveal reaction force in 3D. Subsequently, the 2D force platform was improved to a 3D mini force platform to measure the reaction force of animals (Autumn et al., 2006; Chen et al., 2006; Full et al., 1991; Kram et al., 1998; Lammers, 2007; Weishaupt et al., 2004). Other force transducer techniques have also been developed to measure the reaction force of various animals (Autumn et al., 2000; Liang et al., 2000). An optical birefringence gel technique was introduced (Harris and Ghiradella, 1980; Full et al., 1995) to measure the reaction force, but it is not reliable enough. Unfortunately, our recent systematical studies demonstrated that these measurements reveal the locomotion dynamics but not the reaction force and do not globally reflect the mechanical coordination relationship between each limb of the animal during locomotion. Here we introduce a newly developed force-measuring array (FMA), report some results obtained by the FMA and compare the difference between the reaction forces measured by FMA and those measured by a force platform. Our paper aims to introduce the FMA and to show the difference between measuring methods, thereby revealing the best way to measure the real reaction forces during animal locomotion.

MATERIALS AND METHODS

Animals

Gecko lizards, *Gekko gecko* (Linnaeus), were obtained from a supplier in Guangxi Province, China. They were housed in a room under simulated natural conditions with fresh water and live insects as food, and kept on a natural light cycle. The mean (±s.d.) mass

was 65.4±2.4 g (N=16) and the snout-to-vent length was 140.2±14.1 mm (N=16). Before the experiments began the geckos were trained in two boxes connected by an aisle, which was similar to the aisle of the FMA. A tested gecko was lured or otherwise persuaded to move from one end of the aisle to the black box located at the other end of the aisle.

Experimental system

The experimental system included the force-measuring setup and locomotion observation setup (Fig. 1). The force-measuring setup comprised 16 3D sensors (2 lines×8 sensors) attached to a frame, forming the FMA (Fig. 1, no. 8, inset nos 1–3), a frame (Fig. 1, nos 4–7) to support the FMA, a signal conditioner (Fig. 1, no. 11, National Instruments, Austin, TX, USA), a computer to sample and save data (Fig. 1, no. 14, Dell, Xiamen, China) and connecting cables (Fig. 1, nos 10 and 12). The locomotion observation setup comprised a high speed CCD video recorder (Fig. 1, no. 18, Mikrotron, MC1311, Unterschleissheim, Germany), a tripod to support the high speed camera (Fig. 1, no. 17), two mirrors at 45 deg to the aisle of the FMA to obtain side images during gecko locomotion (Fig. 1, no. 9), a frame for the CCD recording computer (Fig. 1, no. 15, Lenovo, Nanjing, China) and a connecting cable (Fig. 1, no. 16). The force acquisition and image recording were triggered (Fig. 1, no. 13) at the same time. The 3D sensor (Zhang et al., 2007) (Fig. 1, inset no. 2, Institute of Bio-inspired Structure and Surface Engineering, self-made) was made up of T-shaped aluminium alloy. High-resolution foil strain gauges (Model ZF350-1AA-W, ZEMIC, Hanzhong, China) were glued onto the H-shaped zone and optimized by FEM in order to obtain maximum strain in the zone. A load carrier (30×30 mm) was glued on the top of the 3D sensor to mimic the substrate. The full Wheatstone bridge was used to detect the change of resistance.

Calibration of the 3D sensor

The sensors were calibrated by the dead-weight method. Defining F^X, F^Y, F^Z and U^X, U^Y, U^Z as representing the applied loads and voltage change in the corresponding direction, the corresponding regression is:

$$F^X = 0.9141 \times U^X - 0.0445,\ r^2=0.99999,\ N=16,\ F=1.27\times10^5,\ \text{d.f.}=1,14,\ P=4.08\times10^{-36}.$$
$$F^Y = 0.9308 \times U^Y + 1.7200,\ r^2=0.99999,\ N=16,\ F=2.98\times10^5,\ \text{d.f.}=1,14,\ P=1.06\times10^{-31}.$$
$$F^Z = 2.2245 \times U^Z - 1.2738,\ r^2=0.99995,\ N=16,\ F=1.75\times10^5,\ \text{d.f.}=1,14,\ P=4.39\times10^{-37}. \quad (1)$$

The load limit is 1500 mN and the load resolution in the X-, Y- and Z-directions is 2, 2 and 3 mN, respectively.

The sensor was loaded with different dead weights in the X-, Y- and Z-directions (Fig. 2A) and the coefficients C_{ij} in Eqn 2 were determined by regression of the loaded weight and the output of the sensors. Then we fitted the static characteristic curves to lines by the method of least squares and extracted the slope of each fitted line to make up the matrix **C** (Fig. 2B–D). The output of the sensor **U** to the applied load **F** is given by:

$$\begin{pmatrix} U^X \\ U^Y \\ U^Z \end{pmatrix} = \begin{pmatrix} C_{XX} & C_{XY} & C_{XZ} \\ C_{YX} & C_{YY} & C_{YZ} \\ C_{ZX} & C_{ZY} & C_{ZZ} \end{pmatrix} \begin{pmatrix} F^X \\ F^Y \\ F^Z \end{pmatrix}. \quad (2)$$

C_{ij} is the change of electric voltage in the j direction when the load acted in the i direction. The coefficients of the sensors differ somewhat because of their manufacture – therefore all were calibrated. After the sensors were calibrated and the detected voltage variations of each sensor **U** were measured, the applied force **F** acting on the sensor could be obtained by:

$$\begin{pmatrix} F^X \\ F^Y \\ F^Z \end{pmatrix} = \begin{pmatrix} C_{XX} & C_{XY} & C_{XZ} \\ C_{YX} & C_{YY} & C_{YZ} \\ C_{ZX} & C_{ZY} & C_{ZZ} \end{pmatrix}^{-1} \begin{pmatrix} U^X \\ U^Y \\ U^Z \end{pmatrix}. \quad (3)$$

The corresponding coefficients and reverse matrices of one sensor in the above FMA are shown in Eqns 4 and 5:

$$\begin{pmatrix} U^X \\ U^Y \\ U^Z \end{pmatrix} = \begin{pmatrix} -4.4730 & -0.0776 & 0.1254 \\ 0.0441 & -3.5596 & 0.1471 \\ -0.0431 & -0.0269 & -3.5531 \end{pmatrix} \begin{pmatrix} F^X \\ F^Y \\ F^Z \end{pmatrix}. \quad (4)$$

$$\begin{pmatrix} F^X \\ F^Y \\ F^Z \end{pmatrix} = \begin{pmatrix} -0.2234 & 0.0045 & -0.0077 \\ -0.0024 & -0.2570 & -0.0107 \\ 0.0027 & 0.0019 & -0.2813 \end{pmatrix} \begin{pmatrix} U_X \\ U^Y \\ U^Z \end{pmatrix}. \quad (5)$$

The calibration results of all sensors indicate that coupling between different directions is less than 5%. The detailed performance of one of the sensors is given in Table 1, which shows the sensors are good enough for the reaction force measurements.

For dynamic measurement, the natural frequency of the sensor must be high enough to avoid any influence on the measured results (Wu et al., 2010). To achieve this, we refined the geometric structure of the sensor by the finite element method (FEM) to optimize the sensor by increasing the natural frequencies without decreasing the sensitivity. The first order of natural frequency was calculated by FEM as 455, 277 and 589 Hz in the X-, Y- and Z-directions,

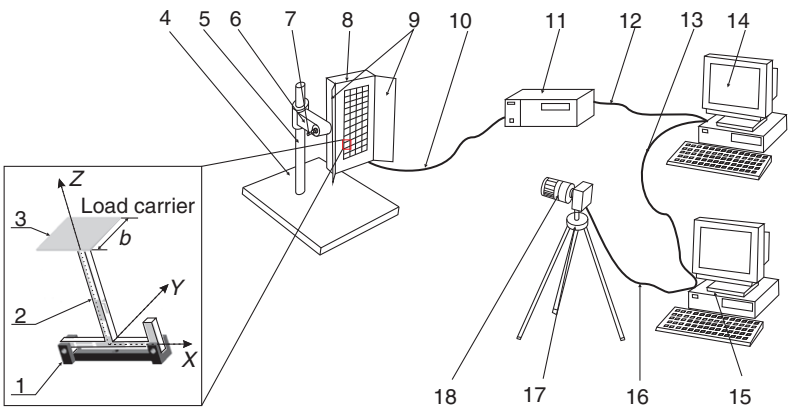

Fig. 1. Setup of the force-measuring array (FMA) and locomotion behaviour observation system. Objects in the figure are as follows: 1, connector linking the 3D sensor to the frame; 2, frame for the sensor; 3, load carrier (b is the width of the load carrier, 30 mm); 4–7, frame supporting the FMA; 8, frame to which the 16 3D sensors are fixed; 9, two mirrors 45 deg to the FMA; 10, 12, 13 and 16, connecting cables; 11, signal conditioner; 14 and 15, computers to sample and save data; 17, tripod to support the high speed camera; and 18, high speed CCD video recorder.

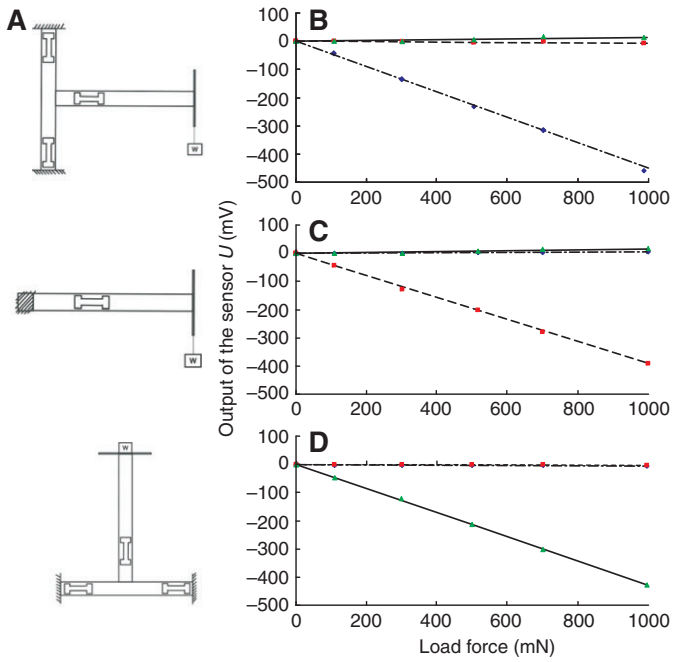

Fig. 2. Calibration of the sensor by the dead-weight method (w, weight). (A) Calibrating the sensor in the *X*-, *Y*- and *Z*-directions; (B–D) regressions of the calibration results corresponding to the *X*-, *Y*- and *Z*-directions, respectively. Red squares, *Y*-direction; green triangles, *Z*-direction; blue diamonds, *X*-direction.

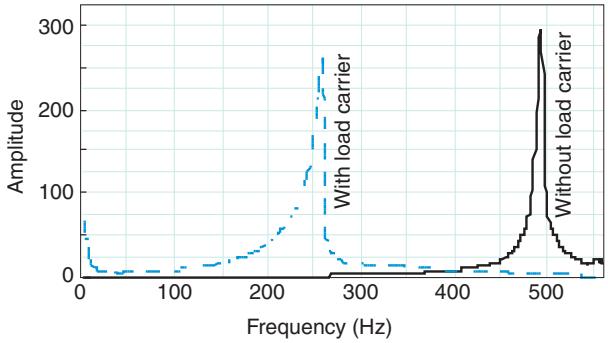

Fig. 3. Measuring the natural frequency of the sensor. The natural frequency was measured by the hammering method in the lateral direction for a sensor with (252 Hz) or without a load carrier (491 Hz).

respectively. The frequency was also measured by a high frequency accelerometer (PCB 352C23, model ICP; PCB Piezotronics Inc., Depew, NY, USA) using the hammering method, which gave values of 491 Hz (Fig. 3), 235 and 561 Hz, respectively. These data are consistent with the FEM calculation. After a load carrier was fixed on the top of the sensor (Fig. 1, inset no. 3), the natural frequencies of the system (sensor with load carrier) were reduced to 252 Hz (Fig. 3 dashed line), 125 and 355 Hz, respectively.

Measuring reaction forces independently and setting the slope substrate

To measure the force acting on each sensor independently, we calculated the deformation of each sensor under maximum load and fixed the sensors into two lines, with a clearance of 1.0±0.1 mm between the load carrier of the sensors and the frame or between neighbouring sensors (Fig. 4A). To measure the reaction forces between the gecko's foot and an inclined substrate, our design allows the FMA and the mirrors (Fig. 4A) to rotate about an axis on the frame, so that the array can be fixed at all angles between the horizontal (slope angle 0 deg) and an upside-down position (slope angle 180 deg).

Recording the locomotion behaviour

We mounted two mirrors on the left and right (Fig. 4A) of the sensor array to enable us to record 3D locomotion behaviours using a high speed camera at 150–500 frames s^{-1} (Fig. 1, no. 18); that is, behaviours in the lateral and fore–aft direction from the real image, and side views in the normal and fore–aft direction from the mirror images (Li et al., 2009). The camera was mounted perpendicular to the sensor array and covered all arrays in the image. One recorded image during a gecko's locomotion is shown in Fig. 4A. The measured force and the recorded image were synchronized by a connected trigger (Fig. 1, no. 13). From the images we were able to check the contact status of the foot on the load carrier of the FMA to select out the corresponding reaction force. The obtained reaction forces are shown in Fig. 4B. Fig. 4C shows the locomotion behaviours and corresponding 3D reaction forces acting on each foot. In order to show the general pattern of the reaction forces, the data presented in Fig. 4C,D were smoothed by 10 Hz.

A force platform to repeat previous measurements

To compare our experimental results with measurements previously reported, we developed a 200×400 mm force platform (Fig. 5A) supported by four 3D sensors (Fig. 1, inset no. 2) to repeat the experiments carried out by Autumn and colleagues (Autumn et al., 2006). The locomotion behaviour in a bird's eye view and two side views was recorded by a high speed video-camera. When a gecko moved along the force platform, the reaction force and locomotion behaviour were synchronously recorded over time. The relationship between reaction force and locomotion behaviour is shown in Fig. 5B.

Experimental methods

We set up the FMA at predetermined slope angles, put a gecko at one end of the aisle and a black box at the other end, and persuaded the gecko to move freely along the aisle of the sensor array and trigger the data acquisition and locomotion recording simultaneously. We carefully checked the reaction force data and the recorded images to select those recordings which met the following conditions: (i) all toes of a foot acting on only one or two sensors; (ii) no slip taking place during the experiment; (iii) no sudden acceleration or deceleration during the test. Such data were saved and numbered.

Table 1. Specification of 3D sensor

Direction	Full scale (FS) (mN)	Resolution (mN)	Non-linearity (%FS)	Hysteresis (%FS)	Creeping (%FS 30 min^{-1})	Integrative error (%FS)
X	1500	2	0.14	0.24	0.21	0.86
Y	1500	2	0.12	0.22	0.26	0.93
Z	1500	3	0.13	0.21	0.25	0.95

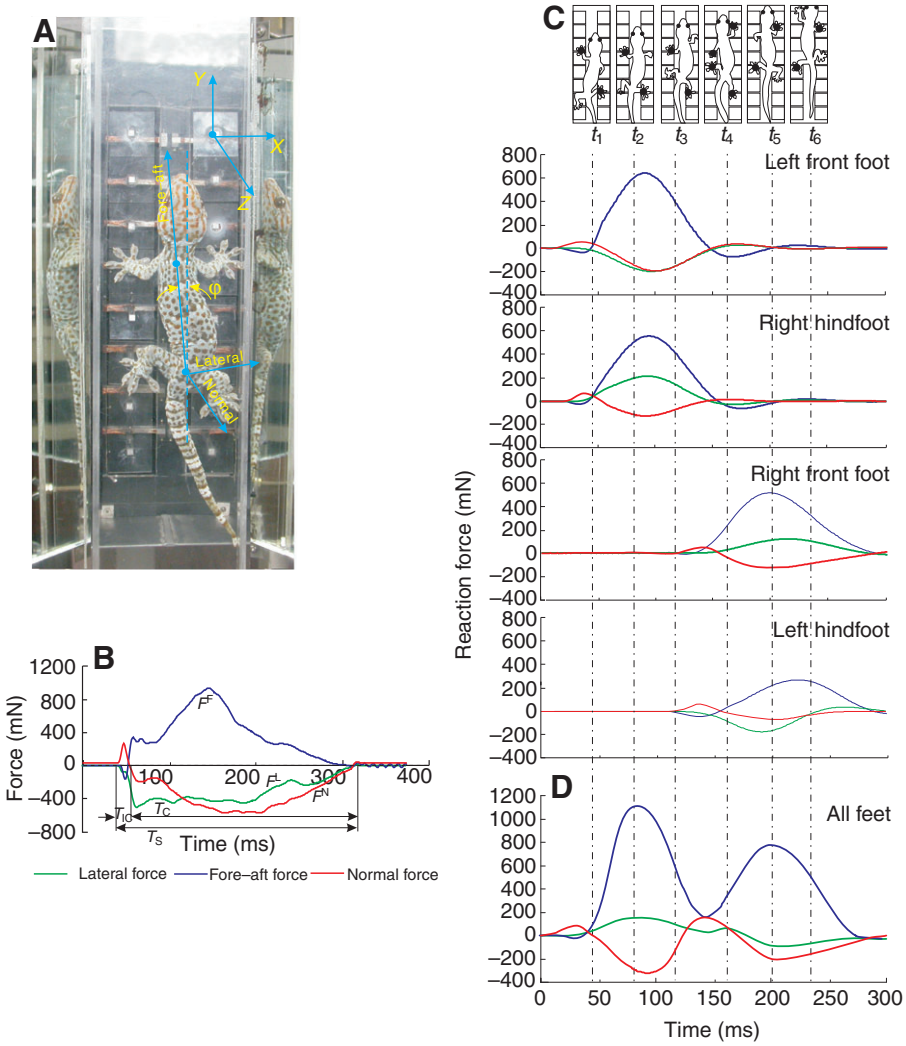

Fig. 4. Locomotion behaviour and reaction forces measured by the FMA. (A) Image recorded by the high speed camera, where sensor-based coordinates (*X*, *Y*, *Z*) and gecko-based coordinates (lateral, fore–aft and normal) are defined and the angle between two coordinates is the transient deflection angle φ. The two side-view images were recorded at the same time. The contact status between foot and load carrier of the sensors was also shown in the images. (B) Reaction force acting on the front left foot by the substrate. F^L, lateral force, F^F, fore–aft force, F^N, normal force. T_{IC}, duration of initial contact – time from the gecko's foot pushing against the sensor to the toe attaching to the sensor; T_C, duration of contact – time from the toe attaching to the sensor to it detaching from the sensor; T_S, duration of contact between gecko's foot or toe and the sensor (T_S=T_{IC}+T_C). (C) Locomotion behaviour and the reaction force acting on each foot during a step cycle. For description of t_1–t_6 see text. (D) The summed reaction forces acting on all feet, which corresponded well with the force obtained by the force platform.

Data calibration

To understand the locomotion dynamics of geckos, the reaction force should be represented by body-based coordinates. During the experiments, the collected reaction forces were represented by sensor-based coordinates; the body-based coordinates may differ from the sensor-based coordinates because the gecko moves on the aisle freely. To minimize the influence of this difference, we converted the reaction force from sensor coordinates to body coordinates. We defined a line from two cross-points of the front limbs and hindlimbs to the dorsal spine, and determined the transient deflection angle φ from this line to the centre line of the array (Fig. 4A). We converted the lateral and fore–aft forces from the sensor coordinates to a gecko body coordinate by the above angle. The force measured by the sensor (F^X, F^Y, F^Z) could be converted into a body coordinate system (F^L, F^F, F^N) by:

$$\begin{bmatrix} F^L \\ F^F \\ F^N \end{bmatrix} = \begin{pmatrix} \cos\varphi & -\sin\varphi & 0 \\ \sin\varphi & \cos\varphi & 0 \\ 0 & 0 & 1 \end{pmatrix} \begin{bmatrix} F^X \\ F^Y \\ F^Z \end{bmatrix}. \quad (6)$$

The shear forces (F^S), over-all reaction forces (F^R), driving angles (α) and support angles (β) were defined by:

$$\left.\begin{aligned} F^S &= \sqrt{(F^L)^2 + (F^F)^2} \\ F^R &= \sqrt{(F^L)^2 + (F^F)^2 + (F^N)^2} = \sqrt{(F^X)^2 + (F^Y)^2 + (F^Z)^2} \end{aligned}\right\}, \quad (7)$$

$$\left.\begin{aligned} \alpha &= \arctan(F^L / F^F) & \alpha &\in (-180°, 180°) \\ \beta &= \arctan(F^N / F^S) & \beta &\in (-90°, 90°) \end{aligned}\right\}. \quad (8)$$

Kinematics

Around 2000 images were obtained for each trial. The locomotion behaviour was represented by two points on the dorsal spine of the gecko; the position (X_i, Y_i) of the marked points on the gecko body was read out from each frame image recorded by a high speed camera. Therefore, the gecko's moving speed (v) was calculated by v_y=(Y_{i+1}–Y_i)/Δt and v_x=(X_{i+1}–X_i)/Δt, where Δt is the time between two images; Y_{i+1}, X_{i+1} and Y_i, X_i are the coordinates of the marked point corresponding to time i+1 and i. Here i is the number of discrete time points. Additionally, the positions of the marked point were used to calculate the transient deflection angle φ.

Data filtering

We set the upper cut-off frequency of Butterworth filtering at 100 Hz in the signal conditioning hardware (National Instruments) after comparing a number of different cut-off frequencies. The collected forces of sensors on which all toes were acting were inputted into Excel (Microsoft) to obtain the maximum lateral force F^L, fore–aft force F^F and normal force F^N during a single foot stance phase, and plotted as graphs (Fig. 4B). The average and divergence of the values were calculated and compared using a t-test.

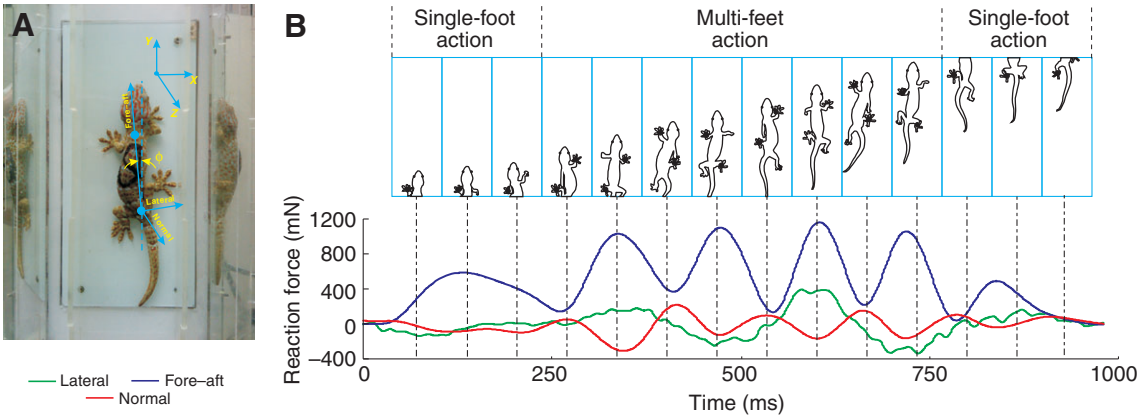

Fig. 5. (A) Illustration of the force platform employed to repeat previous measurements. (B) The locomotion behaviour is shown in the upper section and the forces measured by the force platform are presented in the lower section.

Statistics

An animals' reaction force can be influenced by many factors, such as body weight, excitatory state, locomotion behaviour and environmental condition, so statistical analysis must be introduced to reveal the role of locomotion mechanics. We compared the differences between groups by *t*-test and set the critical *P*-value as 0.05 (SPSS Inc., Chicago, IL, USA). All tested data are presented as means ± s.d.

RESULTS AND DISCUSSION

We set up the FMA and force platform as typical slopes as floor, wall and ceiling and obtained a number of valid trials of the measurements when geckos freely moved on the FMA and on the force platform. We also were fortunate to collect a few groups of data where the four feet of a gecko attached to a sensor consecutively. The following sections will focus on the difference between the reaction force measured by the FMA and by the force platform when the gecko climbs on a vertical substrate in order to find out the best way to measure the reaction forces.

3D reaction force measured by the FMA

When a gecko climbs on a wall, it places its feet on the substrate during T_{IC} and then, attached to the substrate, generates adhesive normal force F^{N}, positive fore–aft force F^{F} and negative lateral force F^{L} during time T_{C} (Fig. 4B).

Fig. 4C shows clearly that the reaction force acting on individual feet by the substrate during a complete step circle is discontinuous. When the gecko climbed on the vertical FMA, the left front foot attached to one load carrier of a sensor first, then the right hindfoot attached to another (Fig. 4C, t_1 black marks). During time $t\in(t_1, t_3)$, the attachment status of feet or under stance phase did not change; the lateral forces acting on the left front foot and the right hindfoot were pulling away from the body in opposite directions, which made the gecko's attachment much more stable. The lateral forces generated counter-clockwise torque, which varied during attachment, with a maximum up to 1.8×10^{-2} N m (around 0.2 N×0.9 m). This torque was balanced by bending of the lateral trunk of the gecko body. The fore–aft forces acting on the left front foot and the right hindfoot were always positive and served to balance the body gravity and drive the gecko upwards on the vertical substrate. The normal reaction force acting on the front foot was negative to generate a torque to prevent the gecko from falling off backwards and the normal force acting on the hindfoot was adhesive or repulsive. The adhesive normal force acting on the hindfoot might be caused by the inertial force of the body in the normal direction. At time $t\in(t_4, t_5)$, the left hindfoot and right front foot gradually attached to the substrate (load carrier of sensor) and the other two feet gradually detached from the substrate. The gecko had performed a transformation of swing phase to stance phase. From t_5 to t_6 the gecko was supported by two legs and preparing for the next phase transformation. To compare the measured data with those obtained by the force platform, we summed the reaction forces acting on all feet (Fig. 4D). The summed lateral force corresponded well to that of results obtained using the force platform (Fig. 5B, multi-feet action). The summed lateral force was much smaller than the corresponding force measured by an individual sensor, which masked the relationship between the locomotion behaviour of lateral trunk bending and the torque generated by lateral forces.

3D reaction force measured by the force platform

Fig. 5B shows the reaction force measured by a force platform with the corresponding locomotion behaviour. When the gecko moved on a vertical substrate, the normal, lateral and fore–aft reaction forces were recorded while only one front foot was attached on the force platform, but then the other front foot attached to the force platform, which resulted in the measured force being a mixture of the reaction forces acting on the two front feet. Therefore it was possible to obtain the maximum reaction force of one foot acting on the substrate, but impossible to obtain a complete recording. When all body weight was supported by the force platform, the measured force fluctuated around its average; the mean of the fore–aft reaction force was the body gravity, while the mean of the normal and lateral forces was around zero. Here, the measured force was not the reaction force, but the inertia force generated by the gecko during locomotion. The biggest variation of fore–aft force corresponded to the change in forward velocity of the gecko body during motion, while the variation of lateral force correlated with trunk bending and swinging of the limbs. When the gecko's front feet moved off the force platform, the reaction force acting on the hindfoot was measured. In short, the force measured by the force platform was only part of the reaction force or the inertia force during the gecko's locomotion. We compared our results with the reaction forces of geckos (Autumn et al., 2006) and cockroaches (Goldman et al., 2006) measured by a force platform, and found the reaction forces *vs* time curves to be similar. All components of the reaction forces – lateral, fore–aft and normal – fluctuated around their average.

When animals moved on a horizontal floor, the measured normal reaction force fluctuated around body weight, but the lateral and fore–aft forces fluctuated around zero (Fig. 5). When animals moved on a vertical substrate, the fore–aft forces changed around body weight, but the other two components varied around zero. The results of our repeated measurements during gecko locomotion revealed the same dynamic response, as the measured force is the inertial force generated during the animals' locomotion. This is because the impact between the animal's foot and a solid substrate, the motion of the legs in swing phase and lateral trunk bending will all cause acceleration and thus generate inertial force. However, all of these measurements do not give the force acting on an individual foot; this force is the key parameter for understanding the locomotion of legged animals because only the force acting on the feet will finally drive the motion of animals.

Comparing the reaction force measured by the two facilities

Comparing the reaction force measured by the FMA and by the mini force platform, it is clear that the results obtained by the FMA more clearly represent the full detailed information from attachment to detachment between an individual foot and a solid substrate, showing reaction forces acting on the foot when it is in stance phase but not when it is in swing phase. We believe the results show the real reaction force acting on the gecko's foot by the environment. On the other hand, the 3D forces measured by the mini force platform fluctuate around their average. The fore–aft force fluctuates around body weight when the gecko climbs vertically, while both normal and lateral forces fluctuate around zero. Thus the reaction force did not follow the physical procedure of stance and swing phase. So the results are the dynamic response of the whole body when the animal moves over the force platform. We are sure that measuring the reaction force using a force platform is not the best procedure, even when a single foot's reaction force can be obtained when the animal's first or last foot acts on the platform, but the reaction force is not complete. We are convinced that, to measure reaction forces properly, the wearable devices and FMA must be introduced.

ACKNOWLEDGEMENTS

We are grateful for support from the National High Technology Research and Development Program of China (grant no. 2007AA04Z201) and National Natural Science Foundation of China (grant nos 60910007 and 50635030).

REFERENCES

Autumn, K., Liang, Y. A., Hsieh, S. T., Zesch, W., Chan, W. P., Kenny, T., Fearing, R. and Full, R. J. (2000). Adhesive force of a single gecko foot-hair. *Nature* **405**, 681-685.

Autumn, K., Hsieh, S. T., Dudek, D. M., Chen, J., Chitaphan, C. and Full, R. J. (2006). Dynamics of geckos running vertically. *J. Exp. Biol.* **209**, 260-272.

Biewener, A. A., Blickhan, R., Perry, A. K., Heglund, N. C. and Taylor, C. R. (1988). Muscle forces during locomotion in kangaroo rats: force platform and tendon buckle measurements compared. *J. Exp. Biol.* **137**, 191-205.

Blickhan, R. and Full, R. J. (1987). Locomotion energetics of the Ghost Crab. II. Mechanics of the centre of mass during walking and running. *J. Exp. Biol.* **130**, 155-174.

Chen, J. J., Peattie, A. M., Autumn, K. and Full, R. J. (2006). Differential leg function in a sprawled-posture quadrupedal trotter. *J. Exp. Biol.* **209**, 249-259.

Dickinson, M. H., Farley, C. T., Full, R. J., Koehl, M. A. R., Kram, R. and Lehman, S. (2000). How animals move: an integrative view. *Science* **288**, 100-106.

Full, R. J. and Tu, M. S. (1990). Mechanics of six-legged runners. *J. Exp. Biol.* **148**, 129-146.

Full, R. J., Blickhan, R. and Ting, L. H. (1991). Leg design in hexapedal runners. *J. Exp. Biol.* **158**, 369-390.

Full, R. J., Yamauchia, D. L. and Jindrich, D. L. (1995). Maximum single leg force production: cockroaches righting on photoelastic gelatin. *J. Exp. Biol.* **198**, 2441-2452.

Goldman, D. I., Chen. T. S., Dudek, D. M. and Full, R. J. (2006). Dynamics of rapid vertical climbing in cockroaches reveals a template. *J. Exp. Biol.* **209**, 2990-3000.

Harris, J. and Ghiradella, H. (1980). The forces exerted on the substrate by walking and stationary crickets. *J. Exp. Biol.* **85**, 263-279.

Heglund, N. C. (1981). A simple design for a force-plate to measure ground reaction forces. *J. Exp. Biol.* **93**, 333-338.

Herzog, W., Nigg, B. M., Read, L. J. and Olsson, E. (1989). Asymmetries in ground reaction force patterns in normal human gait. *Med. Sci. Sports Exerc.* **21**, 110-114.

Kai, M., Aoki, O., Hiraga, A., Oki, H. and Tokuriki, M. (2000). Use of an instrument sandwiched between the hoof and shoe to measure vertical ground reaction forces and three-dimensional acceleration at the walk, trot, and canter in horses. *Am. J. Vet. Res.* **61**, 979-985.

Kleinrensink, G. J., Stoeckart, R., Mulder, P. G. H., Hoek, G. V. D., Broek, T., Vleeming, A. and Snijders, C. J. (2000). Upper limb tension tests as tools in the diagnosis of nerve and plexus lesions Anatomical and biomechanical aspects. *Clin. Biomech.* **15**, 9-14.

Kram, R., Griffin, T. M., Donelan, J. M. and Chang, Y. H. (1998). Force treadmill for measuring vertical and horizontal ground reaction forces. *J. Appl. Physiol.* **85**, 764-769.

Lammers, A. R. (2007). Locomotor kinetics on sloped arboreal and terrestrial substrates in a small quadrupedal mammal. *Zoology* **110**, 93-103.

Li, H. K., Dai, Z. D., Shi, A. J., Zhang, H. and Sun, J. R. (2009). Angular observation of joints of geckos moving on horizontal and vertical surfaces. *Chin. Sci. Bull.* **54**, 592-598.

Liang, Y. A., Autumn, K., Hsieh, S. T., Zesch, W., Chan, W. P., Fearing, R. S., Full, R. J. and Kenny, T. W. (2000). Adhesion force measurements on single gecko setae. Solid-state Sensor and Actuator Workshop, pp. 33-38. Hilton Head Island, SC, USA.

Liu, T., Inouea, Y. and Shibata, K. (2007). Wearable force sensor with parallel structure for measurement of ground-reaction force. *Measurement* **40**, 644-653.

Manter, J. T. (1938). The dynamics of quadrupedal walking. *J. Exp. Biol.* **15**, 522-540.

Merkens, H. W., Schamhardt, H. C., Hartman, W. and Kersjes, A. W. (1986). Ground reaction force patterns of Dutch Warmblood horses at normal walk. *Equine. Vet. J.* **18**, 207-214.

Nikanjam, M., Kursa, K., Lehman, S., Lattanza, L., Diao, E. and Rempel, D. (2007). Finger flexor motor control patterns during active flexion: An in vivo tendon force study. *Hum. Movement Sci.* **26**, 1-10.

Weishaupt, M. A., Wiestner, T., Hogg, H. P., Jordan, P. and Auer, J. A. (2004). Vertical ground reaction force-time histories of sound Warmblood horses trotting on a treadmill. *Vet. J.* **168**, 304-311.

Wu, Q., Ji, A. H., Wang, Z. Y. and Dai, Z. D. (2010). Improvement and test for a force sensor's natural frequency. (In Chinese.) *Chin. J. Sens. Actu.* **23**, 235-238.

Zhang, Z. J., Ji, A. H., Wang, Z. Y. and Dai, Z. D. (2007). 3-Dimensional sensor for measuring geckos ground reaction force. (In Chinese.) *Chin. J. Sens. Actu.* **20**, 1271-1274.